Nigerian Journal of Physics (NJP)
ISSN online: 3027-0936
ISSN print: 1595-0611
DOI: https://doi.org/10.62292/njp.v33i3.2024.278
Volume 33(3), September 2024

Decadal Trend in Humidex: Cooling and Heat Perception in Ibadan, Southwestern Nigeria

*[1]Oluwadare, E. J. and [2]Oluwadare, A. O.

[1]Department of Physics, Faculty of Natural Sciences, Ajayi Crowther University Oyo, Oyo state, Nigeria.
[2]Department of Physical and Chemical Sciences, Faculty of Basic and Applied Sciences, Elizade University Ilara-Mokin, Ondo state, Nigeria.

*Corresponding author's email: ej.oluwadare@acu.edu.ng Phone: +2348061331133

ABSTRACT

Rising global temperatures have resulted in more frequent and intense weather phenomena like heatwaves, storms, and floods, with heatwaves posing notable risks to environment, agricultural and human health. Many studies use localized thresholds to assess heat indexes, taking into account the unique climate patterns of different regions. The Humidex, which measures thermal discomfort, provides a deeper understanding of how temperature and humidity combine to impact human comfort and environmental stress. Weather data from Ibadan, South-Western Nigeria, provided by the Nigerian Meteorological Agency (NIMET), were analyzed for key climate variables to calculate the Humidex. The Mann-Kendall test determined statistical relevance, while Sen's slope measured trend magnitude. Originally developed by Canadian meteorologists, the Humidex assesses how humidity impacts human comfort. The analysis of temperature, relative humidity, and Humidex trends from 2014 to 2023 shows a clear pattern of heat stress during the dry season (February-April) with some relief during the rainy season (June-August). The Mann-Kendall test and Sen's slope revealed a notable downward trend in temperatures, especially in January, March, June, and November, with decreases ranging from -0.08°C to -0.27°C annually. This cooling trend is mirrored by decreasing Humidex values, particularly in January, March and June, indicating reduced heat stress. High humidity levels during the rainy season are mitigated by the cooling effects of rainfall, leading to lower overall heat perception (Humidex). This relationship between temperature and humidity underscores their combined role in influencing heat stress and comfort levels. The annual variations emphasize the importance of monitoring and managing climate risks in regions prone to extreme heat and humidity. Overall, the decline in both temperature and Humidex suggests a shift toward cooler conditions, which could alleviate extreme heat but also prompt concerns about the broader impacts of these changes on regional climate and agriculture.

Keywords:
Humidex,
Temperature,
Humidity,
Trend Analysis,
Heat stress index.

INTRODUCTION

Climate change, driven by global warming, is a paramount issue of the twenty-first century, profoundly impacting various aspects of human life, including public health and agriculture (Andersen, 2006). The increasing global temperatures have led to more frequent and intense weather events such as severe heatwaves, storms, and floods. Heatwaves pose significant threats to both environmental and public health. The expansion and development of urban environments have further exacerbated climatic changes by destabilizing natural environments and adversely affecting the health of urban populations.

Globally, the average annual temperature has risen, and relative humidity has decreased, particularly over land (Denson et al., 2021). Future climate projections indicate continued warming and declining relative humidity, with significant implications for public health and urban sustainability (Byrne and O'Gorman, 2018). The World Health Organization (WHO) has recognized the critical importance of climate's impact on human health, prioritizing the protection of public health against climate change (WHO 2014, Nassiri et al., 2018).

It is well established that discomfort in warm weather is significantly influenced by temperature and humidity levels. Researchers have studied the link between mortality and temperature (Guo et al., 2014). Many studies use location-specific thresholds to assess the heat index, considering the unique weather patterns and geographical characteristics of each area. In recent years, the climate has been marked by an intensifying frequency of extreme heat, impacting human well-being and health. Consequently, the health implications of climate variability have become a critical focus for researchers.

Achieving thermal comfort from a climatological perspective hinges on factors like temperature, humidity, wind, and solar radiation, with temperature and humidity being the most influential for human comfort and health (de Freitas and Grigorieva, 2016). Various indices and models have been developed to assess human thermal comfort, utilizing meteorological data such as air temperature, humidity, wind, and sunlight (Schwingshackl et al., 2021). Thermal comfort indices translate meteorological data into scales that reflect people's responses to weather conditions, ranging from very comfortable to very uncomfortable. These indices simplify the interpretation of atmospheric effects on human comfort and facilitate comparisons between different regions (Esmaeili, 2011).

Heat stress significantly impacts human health, potentially leading to dehydration, heat stroke, and numerous cardiovascular, respiratory, and cerebrovascular diseases (McMichael and Lindgren, 2011; Mora et al., 2017). Heatwaves have been linked to a rise in health issues such as heat rash, heat syncope, muscle cramps, heat exhaustion, and heat shock, and can exacerbate conditions like shortness of breath and tachycardia (Nassiri et al., 2018). These conditions increase the risk of heart attacks and aggressive behaviour, contributing to cardiovascular and cerebrovascular disorders, particularly among older adults (Cheng and Su 2010).

Many meteorological services worldwide have developed systems to warn the public about heat stress dangers (Schwingshackl et al., 2021). Alerts are typically issued when a heat stress index is forecasted to exceed a specific threshold. Examples of heat stress indices include Humidex (Environment and Climate Change Canada, Masterton and Richardson, 1979), Heat index (United States Weather Service, Steadman 1979; Rothfusz, 1990), and the Simplified Wet-Bulb Globe Temperature (Australian Bureau of Meteorology, Buzan et al., 2015).

Humidex is a relatively simple index that relies only on temperature and relative humidity, making it easier to calculate than more complex indices like the Universal Thermal Climate Index and the Wet-Bulb Globe Temperature. Due to its simplicity, Humidex has been adopted in various parts of the world, including Canada (Diaconescu et al., 2022), South Africa (Orimoloye et al.), Iran (Ghalhari et al., 2022), Europe (Scoccimarro et al., 2017), and Italy (Infusino et al., 2021). By combining air temperature and humidity, the Humidex offers a more accurate representation of how weather conditions feel to individuals, particularly in humid environments like those found in many parts of Nigeria.

Extreme weather effects cannot be fully assessed with temperature alone; other indicators such as solar radiation, wind, and relative humidity should be considered for a precise understanding of human health impacts. Immediate surroundings significantly influence wind and solar radiation, with trees, tall buildings and topography reducing wind speed. Likewise, localized events like cloud cover, atmospheric visibility and atmospheric particles reduces the amount of incoming solar radiation. Therefore, wind and radiation are best suited as heat index variables for specific locations due to their significant variability over short distances. In contrast, relative humidity and air temperature are less spatially variable and can indicate thermal comfort over larger areas (Australia Government Bureau of Meteorology 2010).

This study aims to evaluate the changing trends in the Humidex, a measure of thermal discomfort, over a ten-year period from 2014 to 2023 in Ibadan, Oyo State, Nigeria. The study's focus on Humidex adds an important dimension to traditional temperature-based climate studies, offering a nuanced perspective on how climatic factors combine to influence human comfort and environmental stress in the region. This analysis reveals changes in thermal discomfort levels in the region, providing valuable insights into potential impacts on public health and urban planning.

MATERIALS AND METHODS

Description of the Study Area

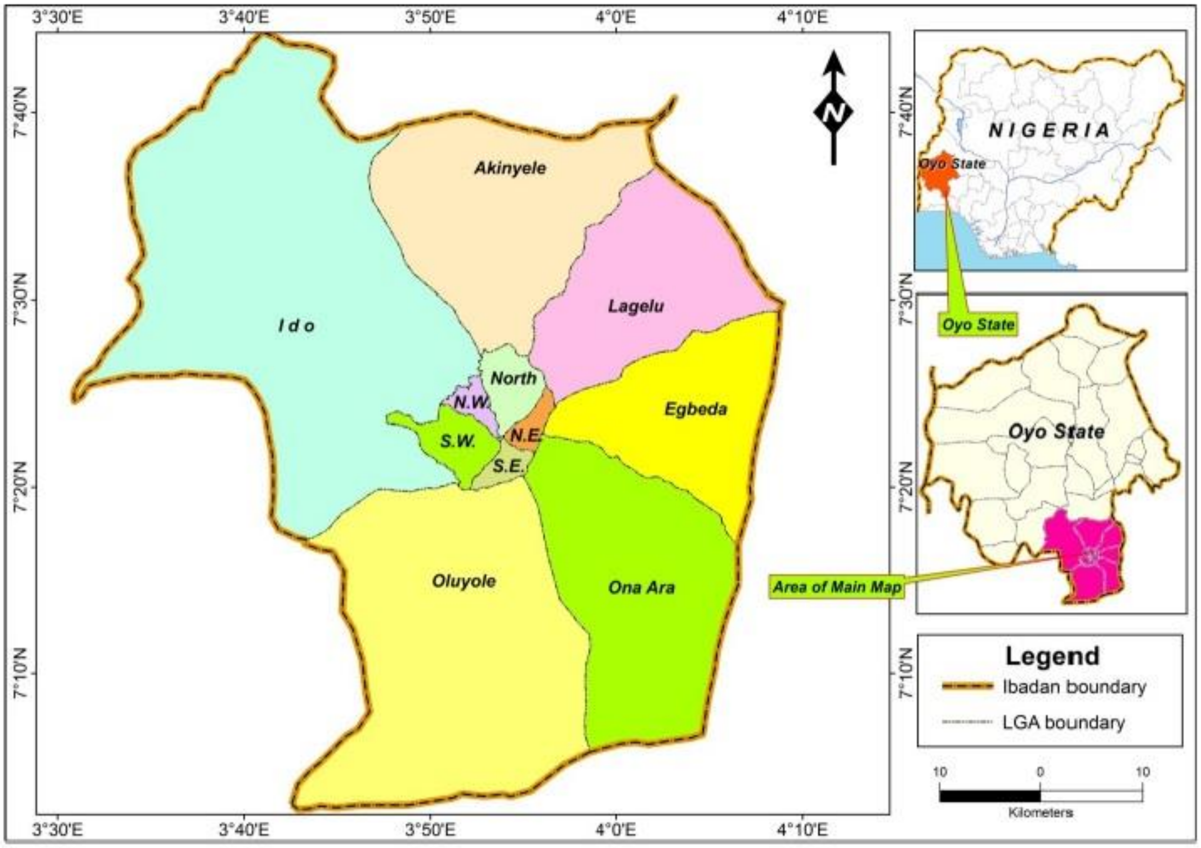

Figure 1: Map of Ibadan, Oyo State, Nigeria. (Source: Adelekan et al., 2020)

Ibadan, the capital and largest city of Oyo State in Nigeria, is one of the country's key urban centres. It ranks as Nigeria's third most populous city after Lagos and Kano. In 1963, Ibadan's population was recorded at 1,141,677, growing at an annual rate of 3.95%. By 1991, this figure rose to 1,829,300, and further increased to 2,550,593 by 2006 (National Population Commission, 2006) Recent estimates from the World Population Review put Ibadan's population at 3,565,108 (World Population Review, 2024).

Geographically, Ibadan is situated between latitudes 7° 02’ 49″ and 7° 43′ 21″ N, and longitudes 3° 31′ 58″ and 4° 08′ 20″ E. Over the years, Ibadan has expanded significantly, making it one of the ten most populous cities in Nigeria, as well as one of the largest in terms of land area. This growth has been driven by its proximity to Lagos, the economic capital of Nigeria, and its status as the capital of the Western Region and later Oyo State after independence (Coker et al., 2008). The city's built-up area has grown from just one square kilometre in the 1830s to 401 square kilometres by 2012 (Adelekan, 2012). Ibadan has a tropical climate with clearly defined wet and dry seasons. The wet season extends from March to October, with the heaviest rainfall in June and September, and a brief dry spell in August. The dry season lasts from November to February, during which the city experiences the harmattan winds common in West Africa. On average, Ibadan receives 1,230 millimetres (48 inches) of rainfall annually, distributed across 123 days. The average daily temperature is 26.46°C, with a mean low of 21.42°C and a relative humidity of 74.55% (Egbinola et al., 2013). The city's elevation varies from 150 meters in its lower regions to 275 meters along the north-south ridge that runs through the city.

Data

This study utilized meteorological data obtained from the Nigerian Meteorological Agency (NIMET) weather station, focusing on key climatic parameters relevant to the calculation of the Humidex. The primary parameters analyzed included air temperature, relative humidity, rainfall, and water vapor pressure, as these factors directly impact the perceived heat and discomfort levels associated with the Humidex index. The meteorological data collected for this study span the period from 2014 to 2023, providing a comprehensive decade-long record of climatic conditions. This extensive dataset allows for a detailed analysis of year-to-year variations in heat stress and perceived temperature, influenced by both temperature and humidity fluctuations.

Data Analysis

The humidex index, created by Canadian meteorologists, was initially used to describe how humidity affects human comfort. On a warm day, high relative humidity can make it feel even hotter because perspiration doesn't evaporate easily. When the humidex value exceeds 40°C, it is considered an extreme weather event (Ho et al., 2016). At a humidex of 30°C, outdoor activities should be carefully managed, paying particular attention to the elderly, children, and the overall health of adults (Rana et al., 2013).

The humidex value represents an equivalent temperature, indicating how hot it feels to the human body by factoring in both temperature and relative humidity. The equation for calculating the humidex was developed by Masterson and Richardson. The humidex index is calculated using equation (1), and the interpretation of its range, from 20 to above 54, is detailed in Table 1.

$$HD = T_a + \frac{5}{9} \times (e - 10) \quad (1)$$

$$e = 6.112 \times 10^{7.5 \times T_a / 237.7 + T_a} \times (RH/100) \quad (2)$$

Where Ta is the air temperature in °C, e is the water vapor pressure in hPa, RH is relative humidity in %.

Table 1: Levels of thermal discomfort associated with different ranges of the Humidex index

Humidex range	Thermal discomfort level
20 - 29	Comfort
30 - 39	Some discomfort
40 - 45	Great discomfort; avoid exertion
46 -54	Dangerous
> 54	Heat stroke possible

Trend Analysis

Trend analysis of a time series involves assessing both the trend's magnitude and its statistical significance. In this study, the statistical significance was evaluated using the non-parametric Mann-Kendall test. Additionally, the trend's magnitude was determined using the non-parametric Sen's estimator method.

Mann–Kendall Test

The Mann-Kendall test evaluates the null hypothesis of no trend against the alternative hypothesis of a monotonic trend in time series. It is suitable for data with a consistent trend and no seasonal patterns. For fewer than 10 data points, S-statistics is used, while Z-statistics is used for 10 or more data points, following a normal distribution (Salmi, 2002). Mann-Kendall statistics (S) is calculated as shown in Equation (3).

$$S = \sum_{i=1}^{n-1} \sum_{j=i+1}^{n} sgn(x_j - x_i) \quad (3)$$

where, x_j and x_i are annual values in years j and i, $j > i$ respectively, n is the length of data series, $i = 1, 2, 3, \ldots n-1$, $j = i+1, i+2, i+3, \ldots n$, and

$$sgn(x_j - x_i) = \begin{bmatrix} 1 \text{ if } (x_j - x_i) > 0 \\ 0 \text{ if } (x_j - x_i) = 0 \\ -1 \text{ if } (x_j - x_i) < 0 \end{bmatrix} \quad (4)$$

If $n \geq 10$, the normal approximation test is used (the Kendall Z-value). The variance of S is then computed using an equation that accounts for ties.

$$Var(S) = \frac{1}{18}\left[n(n-1)(2n+5) - \sum_{p=1}^{q} t_p(t_p - 1)(2t_p + 5)\right] \quad (5)$$

Where, q is the number of tied groups (equal value) and t_p is the number of data values in the p^{th} tied group. The test statistic Z is calculated using the values of S and $VAR(S)$ as follows:

$$Z = \begin{bmatrix} \frac{S-1}{\sqrt{Var(S)}} \text{ if } S > 0 \\ 0 \quad \text{ if } S = 0 \\ \frac{S+1}{\sqrt{Var(S)}} \text{ if } S < 0 \end{bmatrix} \quad (6)$$

A positive Z indicates an increasing trend, while a negative Z indicates a decreasing trend.

The Mann-Kendall test was used to estimate and analyze trend in rainfall time series for the study area for the year 2014 to 2023.

Sen's Estimator Method

Sen's nonparametric method estimates the true slope of a linear trend (Sen 1968).

The slope (T_i) of all data pairs is determined using equation (7)

$$Q_i = \frac{x_j - x_k}{j - k} \quad \text{for i} = 1, 2, 3, \ldots, n \quad (7)$$

Where, x_j and x_k are data values at time j and k, j is subsequent time after time $k(j > k)$.

For time series data with x_j values, the number of slope estimates Q_i is $N = n(n-1)/2$, where n is the number of data points. Sen's estimator of the slope is the median of these N values of Q_i, calculated using equation (8).

$$Q = \begin{bmatrix} Q_{\left[\frac{(N+1)}{2}\right]}, \quad \text{if N is odd} \\ \frac{1}{2}\left(Q_{\left[\frac{N}{2}\right]} + Q_{\left[\frac{(N+2)}{2}\right]}\right), \text{ if N is even} \end{bmatrix} \quad (8)$$

When Q_i is positive, it indicates an increasing trend. Conversely, a decreasing trend shows that Q_i is negative. A zero value of Q_i signifies no trend.

RESULTS AND DISCUSSION

The data in figure 2 shows the monthly temperature trends in Ibadan over a 10-year period (2014-2023). Across all years, the highest temperatures are consistently recorded between February and March, while the lowest temperatures are observed between July and September. Temperatures during the peak months (February-March) are relatively stable, with fluctuations between 28°C and 33°C. However, there is a marked drop in temperatures from June through August, which coincides with the wet season in many tropical regions in Nigeria. While the annual variations are minor, the overall trend shows that 2016 and 2017 had relatively lower average temperatures compared to other years. The temperatures in 2014, 2015, and 2023 indicate relatively warmer conditions compared to mid-decade years (2017-2019). This consistent temperature range suggests that the seasonal weather patterns in the region are driven by larger climatic cycles. The temperature drop during the middle of the year corresponds with the rainy season, which cools the environment.

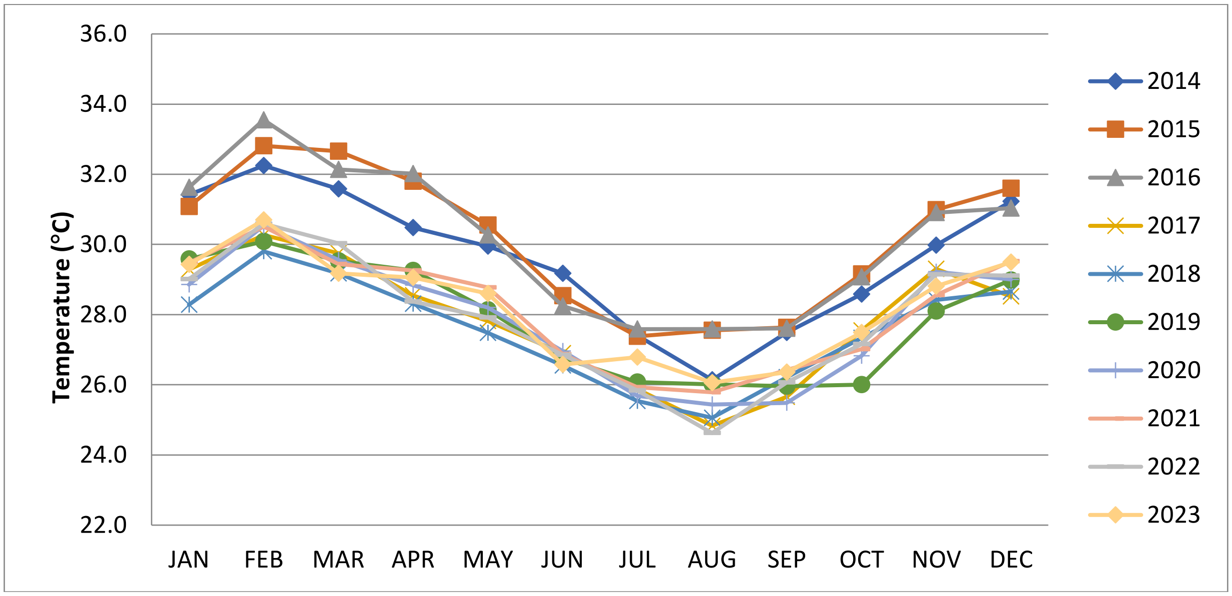

Figure 2: The average monthly temperature (°C) between 2014 and 2023

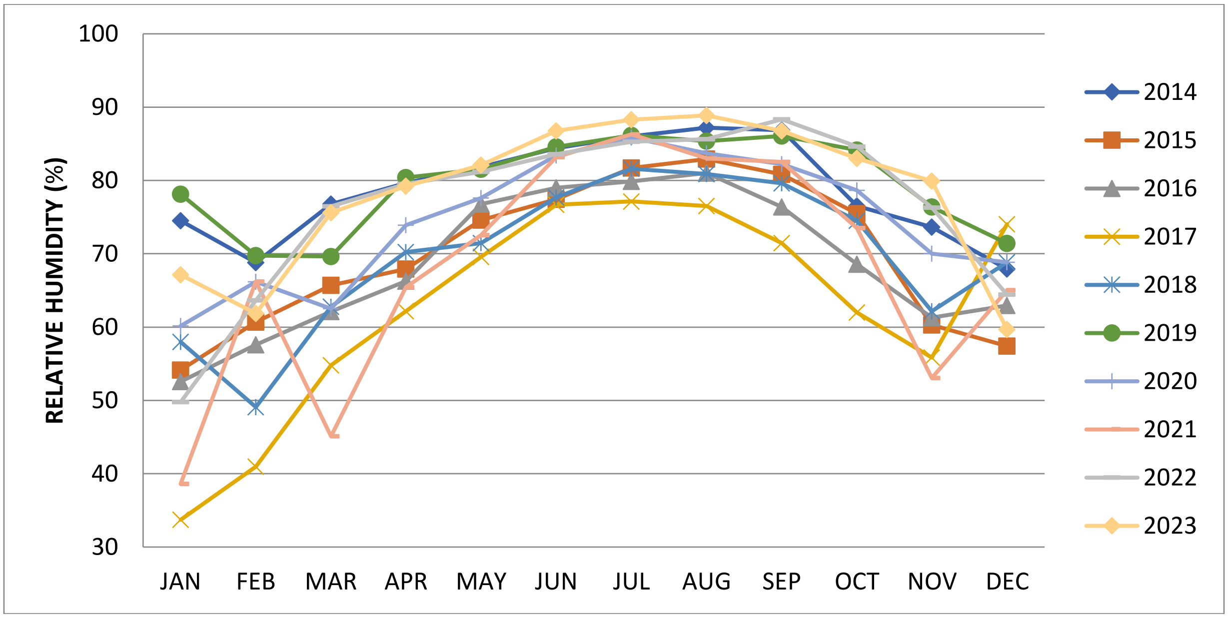

Figure 3: The average monthly relative humidity (%) between 2014 and 2023

The highest humidity levels in Ibadan as shown in Figure 3 occurred during the mid-year months (June to August), coinciding with the rainy season. During this period, relative humidity levels consistently exceed 80%, peaking at around 88% in July and August in recent years (2023). The lowest humidity levels are observed in the beginning and end of each year, particularly in January, February, and December, where humidity drops to as low as 33% (2017) and remains below 60% in many years. These lower humidity levels are typical of the dry Harmattan season. Humidity levels have remained relatively stable across the years, though 2019 and 2023 exhibit notably higher levels, particularly during the mid-year rainy season. The highest humidity levels in 2023 indicate increased moisture content in the air during these periods, while earlier years such as 2017 show much drier conditions in the early months.

Table 2: Average Monthly Humidex (2014-2023)

	JAN	FEB	MAR	APR	MAY	JUN	JUL	AUG	SEP	OCT	NOV	DEC
2014	39.00	40.00	42.09	41.40	40.66	39.16	36.97	35.32	36.82	38.50	40.44	39.37
2015	38.51	41.40	43.49	42.73	41.33	38.56	37.04	36.77	36.90	39.06	41.48	39.77
2016	38.84	42.49	42.92	42.97	41.05	38.25	37.20	36.81	36.82	38.92	41.37	38.88
2017	36.37	37.51	39.82	39.32	38.36	36.88	35.42	34.02	34.93	37.35	39.11	36.36
2018	35.52	37.05	39.28	39.06	38.04	36.53	35.10	34.21	35.44	37.17	38.31	36.13
2019	36.64	37.45	39.70	40.06	38.73	36.69	35.48	35.18	35.17	35.87	38.37	36.31
2020	35.72	38.57	39.96	39.78	38.86	36.91	35.22	34.61	34.72	36.66	39.52	36.70
2021	36.84	38.52	40.03	40.14	39.43	36.81	35.44	34.94	35.73	36.88	38.96	37.60
2022	36.57	38.47	40.58	39.29	38.64	36.84	35.42	33.80	35.40	37.08	39.61	37.26
2023	36.99	38.57	39.73	39.98	39.32	36.57	36.37	35.24	35.69	37.40	39.28	37.64

The highest Humidex values in Ibadan are generally recorded between February and April across all years, indicating that this period tends to feel the hottest due to a combination of high temperatures and elevated humidity. Humidex values during these months often exceed 40, with peaks reaching up to 43.49 in March 2015 and 42.97 in April 2016, indicating potentially uncomfortable or even dangerous heat conditions. From June to August, there is a consistent drop in Humidex values, often to below 37. This reduction coincides with the rainy season, which brings cooler temperatures and higher humidity. Although humidity increases, the overall cooling effect of rain results in lower Humidex values. Over the decade, 2016 and 2015 stand out as having the highest average Humidex values, particularly during the hot months of February through April. In contrast, 2018 and 2019 exhibit lower Humidex readings across most months, particularly in the cooler months like July and August, suggesting milder perceived heat during those years. July and August consistently show the lowest Humidex values (around 35-37), while the months of March and April exhibit the highest perceived heat. For example, in April 2016, the Humidex reached 42.97, making it one of the hottest periods in the decade.

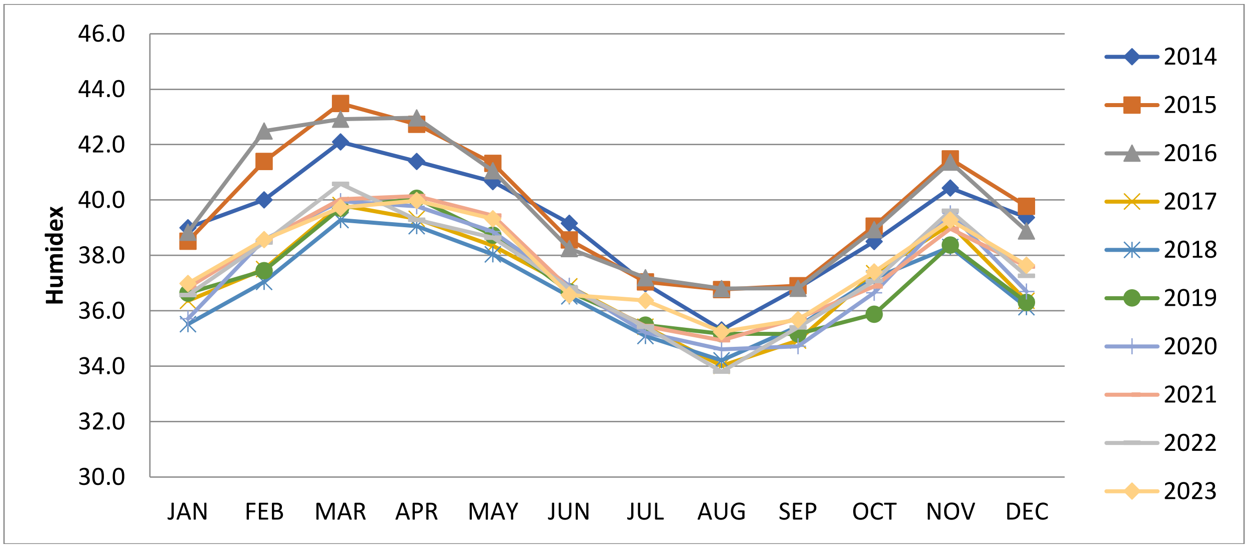

Figure 4: The average monthly Humidex between 2014 and 2023

The line graph in Figure 4 visually represents the same data from Table 2, displaying the monthly Humidex variations in Ibadan over time. The graph shows a clear annual pattern where the Humidex peaks around February to April and then gradually declines through mid-year (June-August), before rising again toward November and December. This pattern reflects the seasonal changes in temperature and humidity in the region. Each year exhibits a similar shape, with significant peaks in March and April, indicating the hottest part of the year. Troughs in July and August demonstrate the cooler, more comfortable months.

The graph allows for easy comparison across years. 2015 and 2016 stand out with higher Humidex values during the hottest months, while 2017 and 2018 show lower peaks, particularly in March and April. The relative uniformity in mid-year Humidex readings suggests that the rainy season exerts a moderating influence on perceived heat across all years.

The consistently high Humidex values between February and April across most years suggest that this period is particularly prone to heat stress, which can affect human health, agriculture, and energy consumption. With values regularly exceeding 40, the perceived heat during these months may pose risks of heat-related illnesses, especially for vulnerable populations.

The drop in Humidex during the mid-year months (June-August) aligns with the rainy season in many tropical regions, which brings cooler temperatures. Although the humidity is high during this time, the rain mitigates the overall heat stress, resulting in lower Humidex values, making these months relatively more comfortable. The yearly variation in Humidex values, particularly in 2015 and 2016, suggests that some years, experience significantly higher heat stress than others. This could be due to changes in atmospheric patterns, such as El Niño or La Niña, which influence weather conditions in tropical regions.

Table 3: Monthly temperature trend for the period (2014 - 2023)

Month	**Mann-Kendall Test (Z)**	**Signific. (α)**	**Sen's slope (Q)**	**Trend**
Jan	-1.43	-	-0.27	↓
Feb	-0.18	-	-0.10	↓
Mar	-1.79	+	-0.27	↓
Apr	-1.25	-	-0.24	↓
May	-0.72	-	-0.17	↓
Jun	-2.33	*	-0.24	↓
Jul	-1.07	-	-0.08	↓
Aug	-0.89	-	-0.11	↓
Sep	-1.07	-	-0.16	↓
Oct	-1.61	-	-0.21	↓
Nov	-1.79	+	-0.20	↓
Dec	-0.36	-	-0.19	↓

↓ = downward trend, signific. = Significance,+ = significant at 99%, * = significant at 90%, - = not significant

Table 3 presents the Mann-Kendall test statistics (Z) and Sen's slope (Q) to assess the monthly temperature trends over the period 2014 to 2023. This test is used to identify trends (upward or downward) in temperature over time. A negative Z-value indicates a downward trend, while a positive value suggests an upward trend. In this case, all Z-values are negative, indicating a consistent downward trend in temperatures across all months, with March, November, and June showing the most significant trends (Z-values of -1.79, -1.79, and -2.33, respectively).

The Sen's Slope (Q) value represents the magnitude of the trend. A negative Q-value across all months further reinforces the fact that temperatures have been gradually decreasing over time. For example, the most significant downward trends are seen in March and January, with slopes of -0.27 and -0.27, respectively, indicating a decline of 0.27°C per year in these months.

The table highlights significant trends, with March, November, and June showing significant downward temperature trends, marked with asterisks (*). These results suggest a 90% confidence level (significant at α = 0.10) that the decrease in temperature is real rather than random.

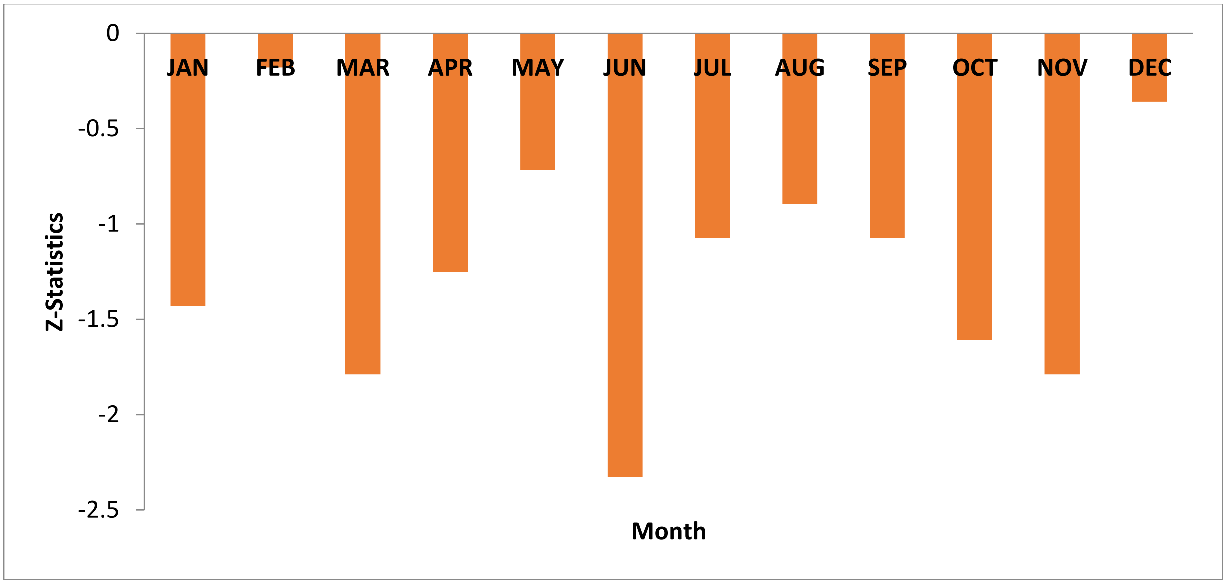

Figure 5: The Mann-Kendall Z -Statistics for Monthly Temperature Trend Analysis

Figure 5 visually represents the Z-statistics from Table 3, illustrating the downward trend in temperature across the months. The graph shows a consistent decline in Z-values, with the lowest Z-scores occurring in June and March. The general downward pattern reflects the cooling trend observed over the study period.

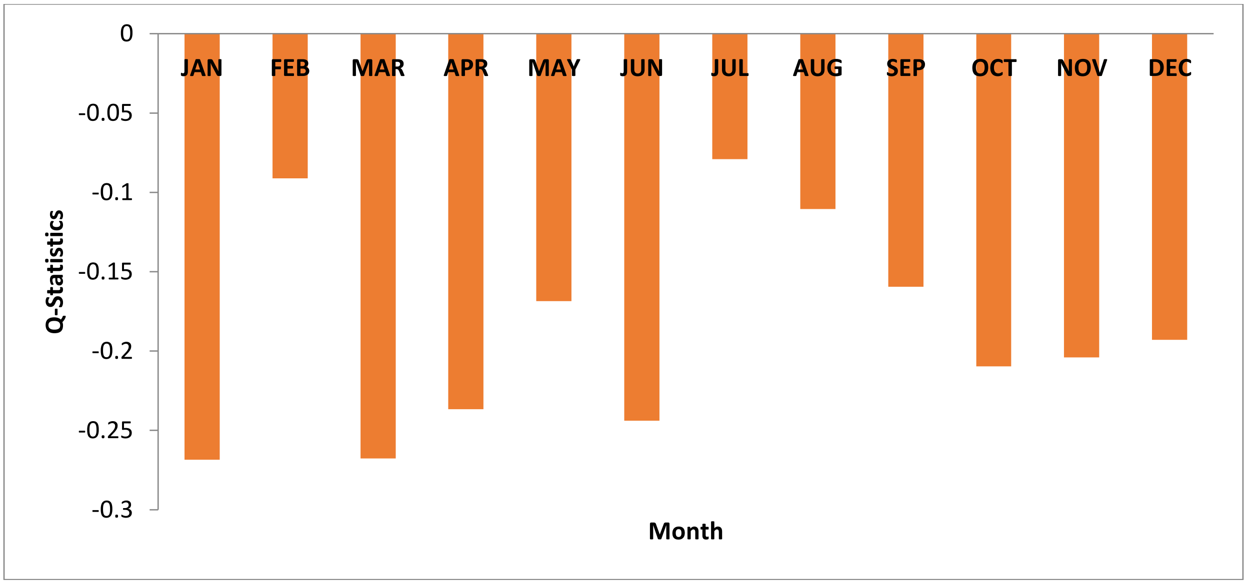

Figure 6: The Sen's Slope (Q) Statistics for Monthly Temperature Trend Analysis

Figure 6 presents the magnitude of the temperature trends, as described by Sen's slope (Q). The figure visually shows the negative values across all months, indicating a cooling trend. The steepest downward slopes are seen in January, March, and June, emphasizing the significant temperature declines during these months.

The data in both Table 3 and Figures 5 and 6 reveal a consistent downward trend in temperatures over the 10-year period. The most significant drops are observed in January, March, and June, which suggests that these months are experiencing more pronounced cooling. This cooling trend may be attributed to various factors, such as changes in atmospheric circulation patterns, increased cloud cover, or other regional climatic changes.

Table 4: Monthly and seasonal Humidex trend for the period (2014 - 2023)

	Mann-Kendall Test (Z)	Signific. (α)	Sen's Slope (Q)	Trend
Jan	-0.89	-	-0.26	↓
Feb	-0.54	-	-0.06	↓
Mar	-0.89	-	-0.26	↓
Apr	-1.07	-	-0.26	↓
May	-0.72	-	-0.18	↓
Jun	-2.15	*	-0.25	↓
Jul	-0.89	-	-0.07	↓
Aug	-0.89	-	-0.12	↓
Sep	-1.25	-	-0.16	↓
Oct	-1.43	-	-0.21	↓
Nov	-0.89	-	-0.15	↓
Dec	-0.54	-	-0.24	↓
Dry Season	-0.36	-	-0.07	↓

↓ = downward trend, signific. = Significance, + = significant at 99%, * = significant at 90%, - = not significant

Table 4 provides an analysis of the Humidex trends, which reflect the perceived temperature based on a combination of actual temperature and humidity. The Mann-Kendall test (Z) and Sen's slope (Q) are used again to assess the trends. Similar to the temperature trend, the Mann-Kendall Test Z-values for Humidex are all negative, indicating a downward trend in the perceived heat. The most significant downward trends are seen in June (Z = -2.15) and September (Z = -1.25), suggesting these months are experiencing cooler perceived temperatures over time. The negative Sen's Slope Q-values again confirm a consistent decline in the Humidex values across all months. The most notable drops are seen in June and March, with slopes of -0.25 and -0.26, respectively, meaning the perceived heat during these months is decreasing by approximately 0.25 units per year. June is the only month with a statistically significant downward trend (at the 90% confidence level), which indicates a strong likelihood that the decrease in Humidex is not random for this month.

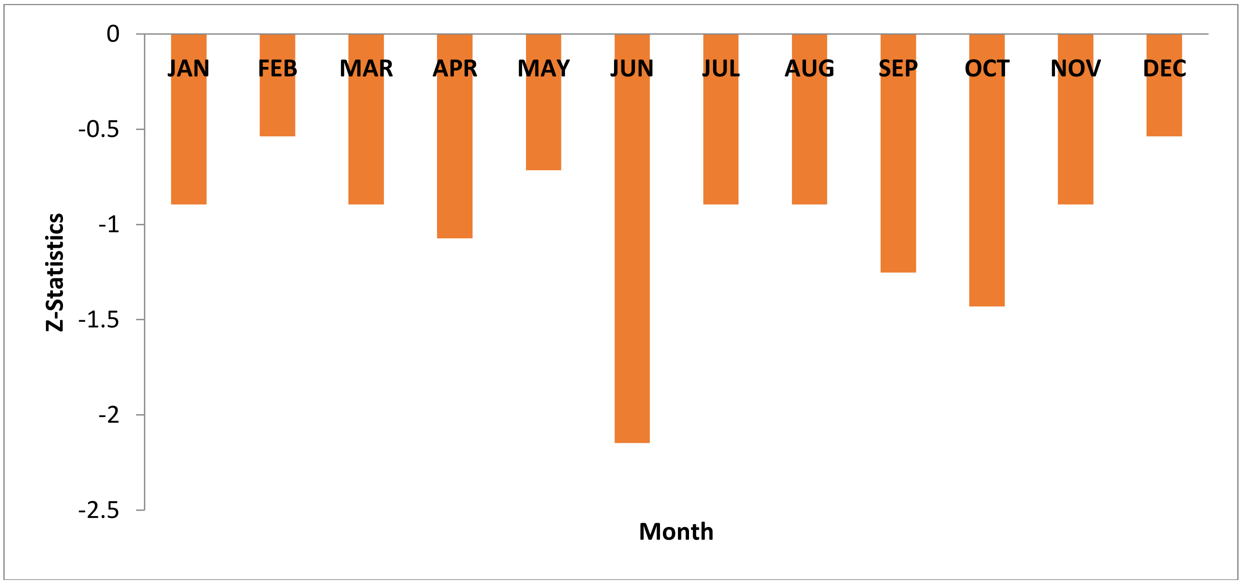

Figure 7: The Mann-Kendall Z -Statistics for Monthly Humidex Trend Analysis

Figure 7 graphically represents the Z-values from Table 4. It shows a general decline in perceived heat (Humidex) across the months, with June, October, and September exhibiting the most significant downward trends. The pattern closely mirrors the temperature trend but with some notable deviations due to humidity's influence on the Humidex.

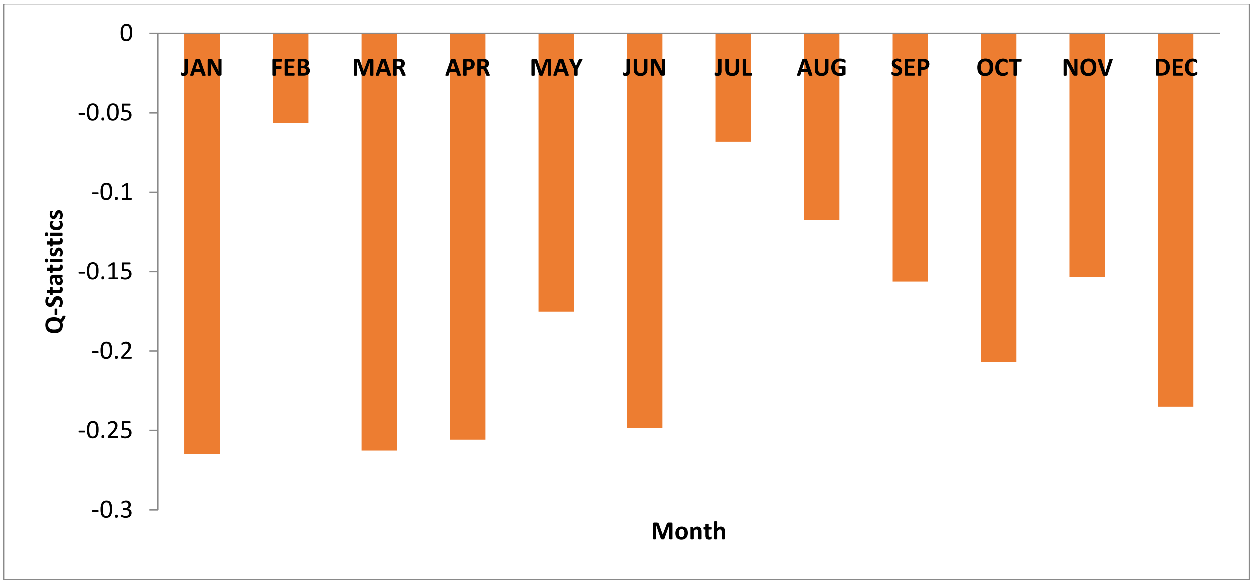

Figure 8: The Monthly Humidex Trend Analysis using Q –Statistics

Figure 8 visually displays the magnitude of the Humidex trends across the months. The negative slopes indicate a reduction in the perceived heat over the study period. The most substantial declines are seen in January, March, and June, again highlighting these months as experiencing the most significant cooling in terms of perceived temperature.

The analysis of Humidex trends shows a consistent decline in perceived heat across the 10-year period. The most significant declines are observed in January, March, and June months that are typically associated with high temperatures and humidity. This suggests that not only is the actual temperature decreasing, but the combination of temperature and humidity is also leading to lower perceived heat levels.

This downward trend in Humidex may provide relief from heat stress, particularly during the hottest months of the year. For agriculture, a lower Humidex could mean reduced heat-related stress on crops, which may improve growing conditions during these months. However, changes in humidity can also have complex effects on evaporation rates, water availability, and plant growth (Scott et al., 2021).

The data in tables 3 - 4 and figures 5 -8 suggest that Ibadan is experiencing a cooling trend in both actual temperature and perceived heat (Humidex) between 2014 and 2023. The most significant cooling is observed in March, June, and November, with noticeable declines in temperature and Humidex values. The cooling trend may have both positive and negative impacts. On the positive side, reduced temperatures and perceived heat can alleviate heat stress for humans and crops, potentially extending the growing season or reducing energy needs for cooling (Hatfield and Prueger 2015). On the other hand, the changes may signal broader climatic shifts, which could alter rainfall patterns or introduce new challenges related to water management and agricultural productivity (IPCC, 2021). Although, from previous research, Egbinola and Amobichukwu (2013) noted that variations in total rainfall and average minimum temperature alone did not conclusively indicate climate change in this region. However, our study of Humidex trends reveals a cooling trend that may suggest subtle shifts in climatic conditions. This finding highlights the importance of using perceived heat indices, like Humidex, as a complementary metric for detecting climate variability. Other studies, such as Scoccimarro et al. (2017) and Infusino et al. (2021), have also demonstrated the value of perceived heat measures in assessing climate impacts across various regions, emphasizing that traditional measures like temperature or rainfall might miss finer variations in human comfort and perceived heat stress. Our results align with this perspective, suggesting that indices sensitive to humidity and perceived heat may better capture local climate nuances, as also underscored by Diaconescu et al. (2022) in similar regional analyses. This approach, combined with conventional climate metrics, could provide a more holistic understanding of climate change impacts, especially in high-humidity regions.

CONCLUSION

The analysis of temperature, relative humidity, and Humidex trends from 2014 to 2023 reveals a clear and consistent cooling trend in both actual temperatures and perceived heat in the region. The Mann-Kendall test and Sen's slope indicate significant downward trends, particularly during key months like March, June, and November, with temperature declines ranging from -

0.08°C to -0.27°C per year. This cooling is reflected in decreasing Humidex values, especially in March and June, suggesting reduced heat stress. Despite high humidity levels during the rainy season, the overall perceived heat is reduced due to the cooling effect of rainfall, highlighting how temperature and humidity together shape the comfort and heat stress experienced by the population. The significant cooling trends in typically hot months like March and June may reduce heat-related stress on humans and crops, yet they could also indicate broader climatic changes that impact seasonal weather patterns, rainfall distribution, and agricultural productivity. Overall, the downward trends in temperature and Humidex suggest a shift towards cooler conditions, potentially offering relief from extreme heat but also raising questions about the long-term effects on regional climate and agriculture. Further monitoring and analysis are essential to understand the drivers behind this cooling trend and its potential consequences.

REFERENCES

Adelekan, I. O. (2012). Vulnerability to wind hazards in the traditional city of Ibadan, Nigeria, *Environ. Urban*. 24 (2) (2012)597–618. http://dx.doi.org/10.1177/0956247812454247.

Adelekan, I., Nwokocha, E. and Olaniyan, F. (2020). *The Role of Local Governments in Reducing Disaster Losses and Vulnerabilities in Ibadan City, Nigeria*. KCL, London; IIED, London.

Andersen, H.E., Larsen, S.E., Hoffman, C.C., Jensen, T.S., Rasmussen, E.K., (2006). Climate-change impacts on hydrology and nutrients in a Danish lowland river basin. *Sci. Total Environ*. 365 (1), 237. https://doi.org/10.1016/j.scitotenv.2006.02.036.

Australia Government Bureau of Meteorology (2010). *Thermal Comfort Observations*. http://www.bom.gov.au/info/thermal_stress/

Buzan, J., Oleson, K. and Huber, M. (2015). Implementation and comparison of a suite of heat stress metrics within the Community Land Model version 4.5. *Geoscientific Model Development*, 8(2), 151–170. https://doi.org/10.5194/gmd-8-151-2015.

Byrne, M.P. and O'Gorman, P.A. (2018). Trends in continental temperature and humidity directly linked to ocean warming. *Proc. Natl. Acad. Sci. USA* 115 (19), 4863–4868. https://doi.org/10.1073/pnas.1722312115.

Cheng X and Su H. (2010). Effects of climatic temperature stress on cardiovascular diseases. *Eur J Intern Med*; 21(3): 164- 7. doi: 10.1016/j.ejim.2010.03.001.

Coker, A. O., Awokola, O. S., Olomolaiye, P. and Booth, C. A. (2008). Challenges of urban housing quality and its associations with neighbourhood environments: Insights and experiences of Ibadan City. *Nigeria. Journal of Environ. Health Research*, 7 (1); 21-30.

de Freitas, C.R. and Grigorieva E.A. (2016). A comparison and appraisal of a comprehensive range of human thermal climate indices. *Int. J. Biometeorol*., 61: 487-512.

Denson, E., Wasko, C., and Peel, M.C., (2021). Decreases in relative humidity across Australia. Environ. Res. Lett. 16 (7), 074023 https://doi.org/10.1088/1748-9326/ac0aca.

Diaconescu E., Sankare H., Chow K., Murdock T. Q., Cannon A. J. (2022): A short note on the use of daily climate data to calculate Humidex heat-stress indices. *Int J Climatol*. 2023;43:837–849. DOI: 10.1002/joc.7833

Egbinola, N. Christiana and Amobichukwu, C. Amanambu (2013). Climate Variation Assessment Based on Rainfall and Temperature in Ibadan, South-Western, Nigeria**.** ***Nigeria Journal of Environment and Earth Science***. Vol. 3, No.11.

Esmaeili, R., A. Gandomkar and M.H. Nokhndan, (2011). Assessment of comfortable climate in several main iranian tourism cities using physiologic equivalence temperature index. *Phys. Geogr. Res. Q*., 75: 8-10.

Ghalhari G. F., Dehghan S. F., Asghari M. (2022). Trend analysis of Humidex as a heat discomfort index using Mann-Kendall and Sen's slope estimator statistical tests. *Environmental Health Engineering and Management Journal*, 9(2), 165-176

Guo, Y., Gasparrini, A., Armstrong, B., Li, S., Tawatsupa, B., Tobias, A., & Tong, S. (2014). Global variation in the effects of ambient temperature on mortality: a systematic evaluation. *Epidemiology (Cambridge, Mass.)*, 25(6), 781.

Hatfield, J. L. and Prueger, J. H. (2015). Temperature extremes: Effect on plant growth and development. *Weather and Climate Extremes*, 10, 4–10. doi:10.1016/j.wace.2015.08.001

Ho, H. C., Knudby, A., Xu, Y., Hodul, M., & Aminipouri, M. (2016). A comparison of urban heat islands mapped using skin temperature, air temperature, and apparent temperature (Humidex), for the greater Vancouver area. *Science of the Total Environment*, *544*, 929-938.

Infusino, E. Caloiero, T. Fusto, F. Calderaro, G. Brutto, A. and Tagarelli, G. (2021). Characterization of the 2017 Summer Heat Waves and Their Effects on the Population of an Area of Southern Italy. *Int. J. Environ. Res. Public Health*, 18, 970. https://doi.org/10.3390/ijerph18030970.

IPCC (2021). Climate Change 2021: The Physical Science Basis. Contribution of Working Group I to the Sixth Assessment Report of the Intergovernmental Panel on Climate Change. Cambridge University Press.

Masterton, J.M. and Richardson, F.A (1979). Humidex: A Method of Quantifying Human Discomfort due to Excessive Heat and Humidity, Canada. *Environment Canada Atmospheric Environment*, Vol. 45.

McMichael, A.J. and Lindgren, E. (2011). Climate change: present and future risks to health, and necessary responses. *Journal of Internal Medicine*, 270, 401–413.

Mora, C., Dousset, B., Caldwell, I.R., Powell, F.E., Geronimo, R.C., Bielecki, C.R., Counsell, C.W.W., Dietrich, B.S., Johnston, E.T., Louis, L.V., Lucas, M.P., McKenzie, M.M., Shea, A.G., Rseng, H., Giambelluca, T.W., Leon, L.R., Hawkins, E. and Trauernicht, C. (2017). Global risk of deadly heat. *Nature Climate Change*, 7, 501–506. https://doi.org/10.1038/nclimate3322.

Nassiri P, Monazzam M R, Golbabaei F, Abbasinia M, Chavoshi M, Taheri F et al. (2018). Exposure to heat stress in the workplace: A systematic review study. *Iran Occupational Health*, 15 (2): 118-28.

National Population Commission (NPC). Nigeria Census Report, 2006.

Orimoloye Israel Ropo, Mazinyo Sonwabo Perez, Nel Werner and Iortyom Enoch T. (2017). Climate Variability and Heat Stress Index have Increasing Potential Ill-health and Environmental Impacts in the East London, South Africa. *International Journal of Applied Engineering Research*, 12 (1), 6910-6918.

Rana, R., Kusy, B., Jurdak, R., Wall, J., & Hu, W. (2013). Feasibility analysis of using humidex as an indoor thermal comfort predictor. *Energy and Buildings*, 64, 17-25.

Rothfusz, L.P. (1990). The heat index equation (or, more than you ever wanted to know about heat index). Forth Worth, TX: NWS S. Reg. Headquarters. Tech. Attachment, SR/SSD 90-23. Available at: https://www.weather.gov/media/ffc/ta_htindx.PDF [Accessed on 29th March 2024].

Salmi, T., Maatta, A., Anttila, P., Ruoho-Airola, T. and Amnell, T. (2002). Detecting Trends of Annual Values of Atmospheric Pollutants by the Mann-Kendall Test and Sen's Slope Estimates—The Excel Template Application MAKESENS. Finnish Meteorological Institute, Publications on Air Quality No. 31, Helsinki.

Schwingshackl, C., Sillmann, J., Vicedo-Cabrera, A.M., Sandstad, M. and Aunan, K. (2021). Heat stress indicators in CMIP6: estimating future trends and exceedances of impact-relevant thresholds. *Earth's Future*, 9(3), e2020EF001885. https://doi.org/10.1029/2020EF001885.

Scoccimarro, E., Fogli, P.G. and Gualdi, S. (2017). The role of humidity in determining scenarios of perceived temperature extremes in Europe. *Environmental Research Letters*, 12(11), 114029. https://doi.org/10.1088/1748-9326/aa8cdd.

Scott, R. L., Knowles, J. F., Nelson, J. A., Gentine, P., Li, X., Barron-Gafford, G., Bryant R., and Biederman, J. A. (2021). Water Availability Impacts on Evapotranspiration Partitioning. *Agricultural and Forest Meteorology*, 297, 108251. https://doi.org/10.1016/j.agrformet.2020.108251.

Sen, P. K. (1968). Estimates of regression coefficient based on Kendall's tau. *Journal of American Statistical Association* 63, 1379 – 1389.

WHO World Health Organization (2014). Quantitative risk assessment of the effects of climate change on selected causes of death, 2030s and 2050s. World Health Organization. Available from: https://apps.who.int/iris/handle/10665/134014.

World Population Review: Nigeria Cities by Population 2024, https://www.world populationreview.com/countries/Nigeria-population/cities. (Accessed 27 September, 2024).